

Coupled-resonator-induced transparency in a fiber system

David D. Smith^{a,b,d,e,*}, N.N. Lepeshkin^b, A. Schweinsberg^b, G. Gehring^b,
R.W. Boyd^b, Q-Han Park^{b,c}, Hongrok Chang^{d,e}, D.J. Jackson^f

^a Department of Physics and Astronomy, The University of New Mexico, Albuquerque, NM 87131, USA

^b The Institute of Optics, University of Rochester, Rochester, NY 14627, USA

^c Department of Physics, Korea University, Seoul, Republic of Korea

^d Department of Physics, University of Alabama in Huntsville, Huntsville, AL 35899, USA

^e Science Directorate, XD42, NASA Marshall Space Flight Center, Huntsville, AL 35812, USA

^f Quantum Computing Technologies Group, Jet Propulsion Laboratory, MS 300-123, 4800 Oak Grove Drive, Pasadena, CA 91109, USA

Received 11 October 2005; received in revised form 11 February 2006; accepted 15 February 2006

Abstract

Mode splitting in two coupled fiber-ring resonators is observed. We observe a cancellation of on-resonance absorption, which can be interpreted as resulting from the destructive interference of the symmetric and anti-symmetric modes of the system, in analogy with electromagnetically-induced transparency in atoms. The response of the system is characterized according to the degeneracy and distinguishability of the normal modes. Finite-difference time-domain simulations agree with an analysis of the transient response of the intra-cavity fields, and reveal coherent oscillations of the photons between the resonators, i.e., under-damped Rabi oscillations, which we predict to occur for distinguishable mode splittings.

© 2006 Elsevier B.V. All rights reserved.

Just as the dipolar response of electrons in an atom can be modeled by a *single* mechanical or electrical oscillator [1], quantum coherence effects in atoms can also be modeled effectively by classical systems of *coupled* oscillators [2–4]. Not surprisingly then, structures composed of two coupled optical resonators have been predicted to display photonic coherence effects such as coupled-resonator-induced absorption (CRIA) and transparency (CRIT) [5,6] in direct analogy with electromagnetically-induced absorption [7] and transparency [8,9] in driven three-level atomic systems. These phenomena were later observed in the whispering-gallery modes of coupled fused-silica microspheres [10], which can possess intrinsic quality-factors exceeding 10^8 . Coherently coupled optical resonators are therefore promising for applications such as optical delay lines [11,12], buffers [13,14], gyroscopy [15–18], optical computing schemes [5], and the modeling of quantum-

mechanical effects in atoms [19–21]. In this paper we experimentally demonstrate coupled-resonator-induced transparency (CRIT) in coupled fiber ring resonators. These systems have the advantage that the coupling between resonators is significantly easier to control than that between micro-resonators, and that the resonators are easily assembled from commercial off-the-shelf components.

The steady-state response of two coupled-resonators, one of which is coupled to an excitation waveguide as shown in Fig. 1, can be readily solved by iterative or matrix techniques [22–24]. We consider incident light whose pulse lengths are longer than the transient response of the structure (the input is quasi-monochromatic). The complex electric-field transmission ($E_{\text{out}}/E_{\text{in}}$) across such a structure is given by the Airy expression

$$\begin{aligned} \tau_2(\phi_1, \phi_2) &\equiv \frac{E_{\text{out}}}{E_{\text{in}}} = r_2 - \frac{r_2^2}{r_2} \sum_{n=1}^{\infty} (r_2 a_2 \tau_1(\phi_1) e^{i\phi_2})^n \\ &= \frac{r_2 - a_2 \tau_1(\phi_1) e^{i\phi_2}}{1 - r_2 a_2 \tau_1(\phi_1) e^{i\phi_2}} = |\tau_2| \exp[i\phi_2^{(\text{eff})}], \end{aligned} \quad (1)$$

* Corresponding author.

E-mail address: david.d.smith@nasa.gov (D.D. Smith).

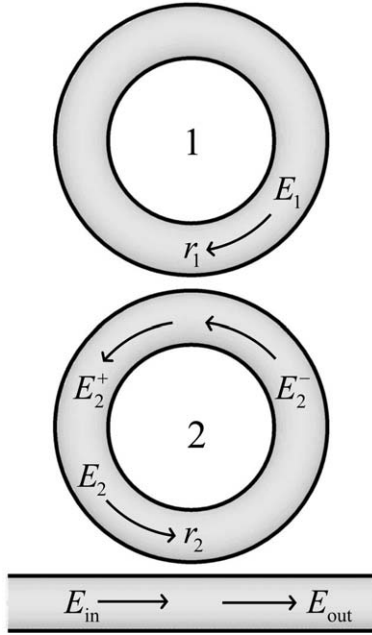


Fig. 1. Electric field designations for two coupled ring resonators.

where

$$\begin{aligned} \tau_1(\phi_1) &\equiv \frac{E_2^+}{E_2^-} = r_1 - \frac{r_1^2}{r_1} \sum_{n=1}^{\infty} (r_1 a_1 e^{i\phi_1})^n = \frac{r_1 - a_1 e^{i\phi_1}}{1 - r_1 a_1 e^{i\phi_1}} \\ &= |\tau_1| \exp \left[i\phi_1^{(\text{eff})} \right] \end{aligned} \quad (2)$$

is the complex transmittivity through the first resonator, $\phi_j = 2\pi n_j L_j / \lambda_0 = \omega_j \tau_j^{(\text{RT})}$ are the single-pass phase-shifts, r_j and t_j are the coupler reflection and transmission coefficients, respectively, $a_j = \exp(-\alpha_j L_j / 2)$ are the single-pass attenuation coefficients, n_j are the refractive indices, α_j are the loss coefficients, L_j are the circumferences of the resonators, the electric fields E_2^- (just before) and E_2^+ (just after) the coupler are shown in Fig. 1, and $j = 1, 2$ specifies the first (furthest from the excitation waveguide) or second (closest to the waveguide) resonator. Note that the angular resonance frequencies ω_j are related to the single pass phase shifts according to $\phi_j = \omega_j \tau_j^{(\text{RT})}$, where $\tau_j^{(\text{RT})}$ are the round-trip times of the resonators. Hence ϕ_j is indicative of the detuning of the input frequency from the resonance frequency. The effective transmitted instantaneous phase shift $\phi^{(\text{eff})}$ and its derivative $d\phi^{(\text{eff})}/d\phi$ are analogous to the single-atom phase and group refractive indices, respectively. When the resonators have identical optical path lengths (they are co-resonant), we can drop the subscript from the single-pass phase shifts. Note that Eq. (1) can also be written as $\tau_2 = \exp[i\tilde{\phi}_2^{(\text{eff})}]$, where $\tilde{\phi}_2^{(\text{eff})} = \phi_2^{(\text{eff})} - i \ln |\tau_2|$ is the complex effective phase shift and is analogous to the single-atom complex refractive index. This single variable $\tilde{\phi}_2^{(\text{eff})}$ thus contains all the information necessary for determining the response of the coupled-resonator structure.

For the case of a single resonator, Eq. (2) displays a *minimum* at resonance ($\phi_1 \bmod 2\pi = 0$), and critical coupling

($T_1 = 0$) occurs at $\phi_1 = 0$ when $r_1 = a_1$. In contrast, consider the case of two coupled resonators, having identical OPLs such that $\phi_1 = \phi_2 = \phi$ (analogous to a degenerate atomic Λ system). Now, if the first resonator is overcoupled ($r_1 < a_1$) then $\phi_1^{(\text{eff})} = \pi$ (the resonators interfere destructively) such that Eq. (1) becomes $\tau_2(0) = (r_2 + a_2 |\tau_1|) / (1 + r_2 a_2 |\tau_1|)$, which displays a *maximum* at the single-ring resonances ($\phi \bmod 2\pi = 0$). As a result, the spectrum is split into symmetric and antisymmetric normal modes, characteristic of induced transparency. The approximate frequencies of the split modes upon transmission ϕ_{sp} can be found by noting that $\text{Im} \tau_2 = 0$ at $\phi = \phi_{\text{sp}}$, provided the change in $\text{Re} \tau_2$ is small at this same frequency:

$$\phi_{\text{sp}} = q2\pi \pm \cos^{-1} \left(r_1 \left[1 + \frac{(1 - a_1)^2}{2a_1} \right] \right). \quad (3)$$

Thus, the transmittance at the split modes is given by

$$T_2(\phi_{\text{sp}}) = \left| \frac{r_2 - a_2 a_1}{1 - r_2 a_2 a_1} \right|^2 \quad (4)$$

and critical coupling (for the structure as a whole) occurs at $\phi = \phi_{\text{sp}}$ when $r_2 = a_1 a_2$. At critical coupling, the transmittance T_2 at $\phi = \phi_{\text{sp}}$ becomes zero. For completeness, we note that induced transparency can also occur when the first resonator is under-coupled ($r_1 > a_1$) such that $\phi_1^{(\text{eff})} = 0$ (the resonators interfere constructively), but in this case the dip in absorption is considerably less dramatic.

The intracavity electric fields are determined in a fashion similar to the transmittivities [23], by a summation of the contributions from the multiplicity of round trips. We make a subtle, yet important, distinction between what we refer to as cavity buildup and magnification factors. The buildup factor is the ratio of the internal field in a particular resonator to the input to that same resonator, whereas the magnification factor is ratio of the internal field to the input to the entire structure. The electric-field buildup factors are given by

$$\beta_1(\phi_1) \equiv \frac{E_1}{E_2} = i t_1 a_1 e^{i\phi_1} \sum_{n=0}^{\infty} (r_1 a_1 e^{i\phi_1})^n = \frac{i t_1 a_1 e^{i\phi_1}}{1 - r_1 a_1 e^{i\phi_1}} \quad (5)$$

and

$$\begin{aligned} \beta_2(\phi_2, \phi_1) &\equiv \frac{E_2}{E_{in}} = i t_2 a_2 \tau_1 e^{i\phi_1} \sum_{n=0}^{\infty} (r_2 a_2 \tau_1 e^{i\phi_2})^n \\ &= \frac{i t_2 a_2 \tau_1(\phi_1) e^{i\phi_2}}{1 - r_2 a_2 \tau_1(\phi_1) e^{i\phi_2}}, \end{aligned} \quad (6)$$

where the internal fields E_1 and E_2 are shown in Fig. 1. The intensity buildup factors are then given by $B_j = |\beta_j|^2$. The electric-field magnification factors are related to the buildup factors by the relations

$$\mu_2(\phi_1, \phi_2) \equiv \frac{E_2}{E_{in}} = \beta_2(\phi_1, \phi_2) \quad (7)$$

and

$$\mu_1(\phi_1, \phi_2) \equiv \frac{E_1}{E_{in}} = \frac{\beta_2(\phi_1, \phi_2)\beta_1(\phi_1)}{\tau_1(\phi_1)a_{22}} e^{-i\phi_{22}}, \quad (8)$$

where a_{22} and ϕ_{22} represent the attenuation and phase shift during the clockwise propagation from the first coupler back to the second, respectively. The relationship between the magnification factors is then clearly

$$\begin{aligned} \frac{\mu_1(\phi_1, \phi_2)}{\mu_2(\phi_1, \phi_2)} &= \frac{|\mu_1(\phi_1, \phi_2)|}{|\mu_2(\phi_1, \phi_2)|} e^{-i\Delta\phi^{(eff)}} \\ &= \frac{i t_1 a_1 e^{i\phi_1}}{[r_1 - a_1 e^{i\phi_1}] a_{22}} e^{-i\phi_{22}}, \end{aligned} \quad (9)$$

such that the effective phase difference between the intra-cavity fields is

$$\begin{aligned} \Delta\phi^{(eff)} &\equiv \text{Arg} \left[\frac{\mu_1(\phi_1, \phi_2)}{\mu_2(\phi_1, \phi_2)} \right] \\ &= \left[\phi_1 - \phi_{22} + \frac{\pi}{2} \right] - \text{Arg}[r_1 - a_1 e^{i\phi_1}]. \end{aligned} \quad (10)$$

The effective phase difference vs. the single-pass phase-shift is plotted in Fig. 2. The intra-cavity fields are in phase for the symmetric lower-energy mode, whereas they are out-of-phase for the anti-symmetric higher-energy mode. This result is also observed in the finite-difference time-domain (FDTD) simulations. The energy difference is due to the different strength of the electric field in the dielectric material of the coupler which polarizes it to a different degree.

The complex poles of the transmittivity in Eq. (1) are simply the complex eigenmodes of the coupled resonator system

$$\begin{aligned} \tilde{\phi}_2^{(\text{poles})} &= \phi_{\pm} - i \frac{\gamma_{\pm}}{2} \\ &= -i \left(\frac{1}{2} \ln \frac{1}{r_2 a_1 a_2} + \ln \left\{ \frac{r_1}{r_1^{(ep)}} \pm \left[\left(\frac{r_1}{r_1^{(ep)}} \right)^2 - 1 \right]^{1/2} \right\} \right), \end{aligned} \quad (11)$$

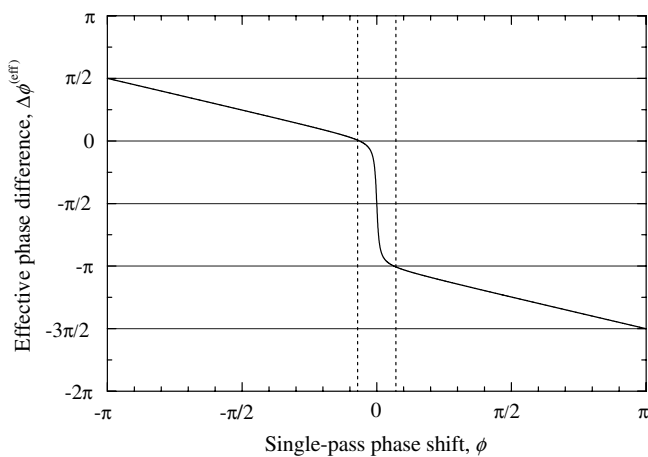


Fig. 2. The effective phase difference between the intra-cavity fields vs. the single-pass phase shift.

where ϕ_{\pm} and γ_{\pm} are associated real-valued frequencies and linewidths. The eigenmodes are completely degenerate, i.e., the frequencies and linewidths of the split modes are identical ($\phi_+ = \phi_-$ and $\gamma_+ = \gamma_-$), at the exceptional point

$$r_1^{(ep)} = \frac{2(r_2 a_1 a_2)^{1/2}}{a_1 + r_2 a_2}. \quad (12)$$

The linewidths are degenerate ($\gamma_+ = \gamma_-$) for $r_1 < r_1^{(ep)}$ (over-exceptional couplings), whereas the frequencies are degenerate ($\phi_+ = \phi_-$) for $r_1 > r_1^{(ep)}$ (sub-exceptional couplings). A complete degeneracy in both frequency and linewidth is obtained only at the point $r_1 = r_1^{(ep)}$. Note that the exceptional point depends on the magnitude of the coupling in comparison with the differential loss. When $a_1 = r_2 a_2$ there is no differential loss, and $r_1^{(ep)} = 1$, i.e., the frequency splits (over-exceptional) for any value of the coupling. In addition, the eigenmodes can be characterized according to their distinguishability. The modes are referred to as distinguishable when the frequency splitting is larger than the average linewidth, i.e., when $\phi_+ - \phi_- > (\gamma_+ + \gamma_-)/2$. This occurs when $r_1 < r_1^{(dist)}$, where

$$r_1^{(dist)} = r_1^{(ep)} \cos \left(\frac{1}{2} \ln \frac{1}{r_2 a_1 a_2} \right) \quad (13)$$

is the distinguishable point. Note that in the limit of small resonator losses, i.e., for $r_2 a_1 a_2 \approx 1$, we obtain $r_1^{(dist)} = r_1^{(ep)}$, i.e., one can distinguish degenerate eigenmodes only at the point where the linewidth goes to zero, the transmission becomes infinite, and zero splitting is just resolvable, i.e., at the lasing threshold.

It turns out that the coupling required to distinguish the eigenmodes $r_1 < r_1^{(dist)}$ is identical to that required for the observation of under-damped Rabi oscillations. For smaller couplings the oscillations are overdamped. The simplest way to understand this is to invoke the coupled mode approximation. For input pulses long compared to the structural response time, the comb part of the impulse response is washed out. Moreover, for sufficiently large resonator quality factors (the limit of small losses), and weak coupling between the resonators, coupled mode equations provide a good approximation for the structural response. Because the coupled mode equations are formally identical to the Schrödinger equation in the rotating-wave approximation (RWA), under these conditions the response is characterized to a good approximation by that of the well-known damped Rabi problem [25,26]. But, in this case nutation involves the exchange of photons between resonators, rather than population between atomic energy levels. In the presence of differential loss, i.e., when $a_1 \neq r_2 a_2$, the Hamiltonian is non-Hermitian and there is energy exchange between the split modes (dressed states), since they are no longer the true eigenmodes (which are now complex) of the system. Rabi oscillations are observed when the coupling is large enough in comparison with the differential loss that frequency splitting occurs in the intracavity field of both resonators. Essentially, in this case the observed

split modes (dressed states) sufficiently approximate the eigenmodes of the system, such that very little energy is exchanged between them, and they remain distinguishable. For smaller couplings the intracavity frequency splitting occurs only in the second resonator. In this case the split modes (dressed states) are indistinguishable and exchange significant energy with each other, since they no longer adequately approximate the eigenmodes of the system. Hence, in this case, Rabi oscillations do not occur between the resonators (bare states) because they are over-damped by the differential loss. These observations are particularly relevant in laser gyroscopy. Rabi oscillations have been observed to occur in laser gyroscopy experiments as the result of intra-cavity rather than inter-cavity coupling [16,20,21]. The presence of underdamped Rabi oscillations indicates that the observed beat-note is strongly determined by the coupling, rather than by the rotation itself. Distinguishability of modes (standing waves in the case of a gyro) is thus closely related to the sensitivity of a laser gyro [27]. In the experiments described below the coupling

varies through the distinguishability point, such that both distinguishable and indistinguishable splittings are observed.

The temporal response can be determined either using the impulse response function, or using the approximation of the coupled mode equations. The results of this analysis are shown in Fig. 3a, where the internal intensity magnification factors $M_j = |\mu_j|^2$ for the two resonators are plotted as a function of time. Under-damped Rabi oscillations are observed in these results, as well as in the FDTD simulation in Fig. 3b. Note that at $\phi = \phi_{sp}$ the factors M_1 and M_2 are identical. At $\phi = 0$, however, they are considerably different. Initially, as the resonators fill, more photons occupy the bottom ring. In the steady-state, however, more photons occupy the upper ring, i.e., the photons appear to be trapped or to tunnel into the upper ring. This situation is analogous to a population inversion in a two-level atom, coherent population trapping in three-level systems, and/or quantum mechanical tunneling phenomena.

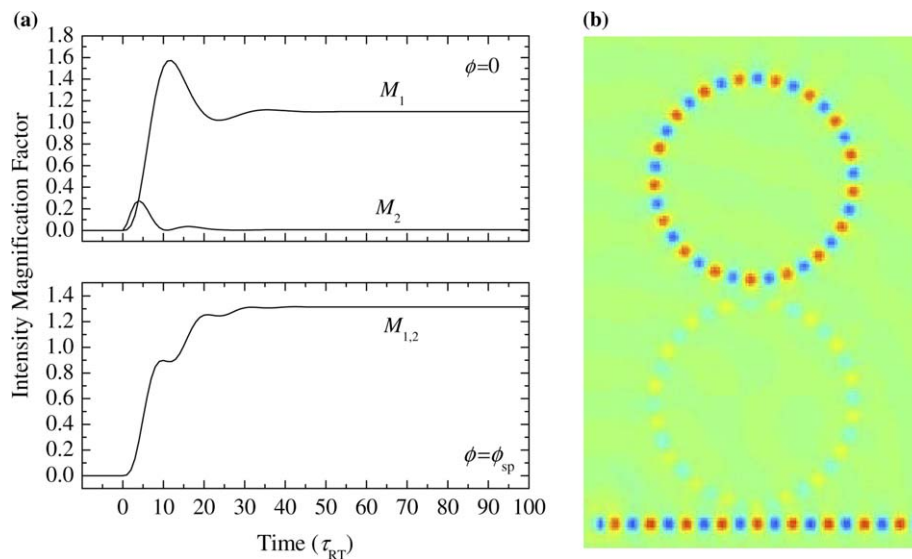


Fig. 3. Temporal response of coupled resonators: (a) internal intensity magnification factors at $\phi = 0$ and $\phi = \phi_{sp}$; (b) FDTD simulation with a monochromatic input at $\phi = 0$.

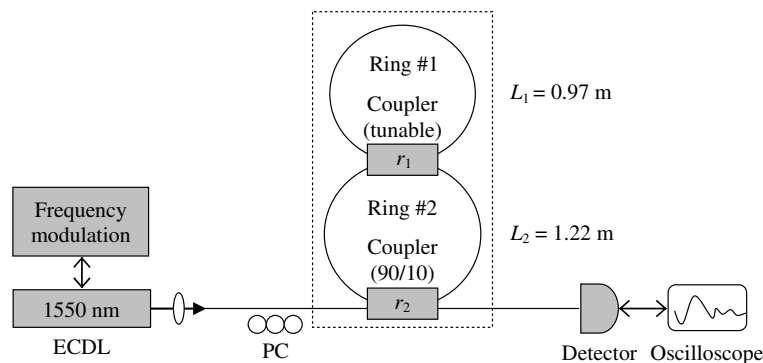


Fig. 4. Experimental setup for observation of CRIT in an all fiber system.

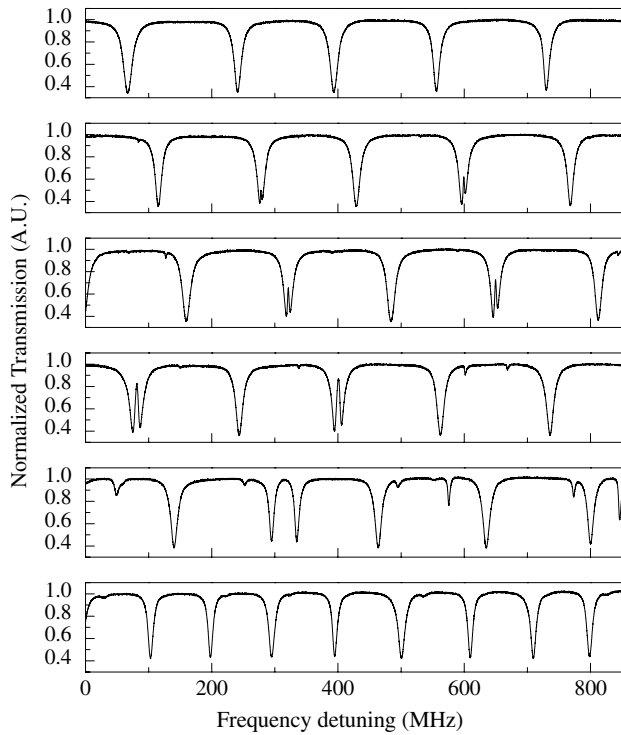


Fig. 5. Mode splitting in the transmission spectrum of two coupled fiber ring resonators. The couplings are $r_1 = 1.0, 0.999, 0.995, 0.99$ (indistinguishable), and $r_1 = 0.96, 0.1$ (distinguishable) from top to bottom. The fixed parameters are: $a_1 = 0.98, a_2 = 0.82,$ and $r_2 = 0.95$.

The experimental setup of interest is shown in Fig. 4. A tunable external-cavity diode laser operating at 1550 nm was used to probe the transmission of a system consisting of two coupled fiber rings, $L_1 = 1.22$ m and $L_2 = 0.97$ m in circumference. The laser output was isolated and end-fire coupled into a straight section of a single-mode fiber which was weakly coupled to one of the rings by means of a 90/10 coupler. A polarization controller was used to select TE polarization. The two rings were inter-coupled by a tunable coupler and submerged into a water bath for thermal stabilization.

The output was detected with an InGaAs PIN photodiode, and recorded on a digital storage oscilloscope as the laser was scanned over a frequency range spanning several resonances (typically 1 GHz) at a scan rate of several hundred hertz. Whispering-gallery modes were initially observed in the second ring (the innermost ring, closest to the excitation guide), with the first ring being de-coupled from the system. Then, changes in the resonances were observed as the coupling between the rings was increased as shown in Fig. 5, which shows the transmission of the system as a function of laser detuning for a variety of couplings. In the trace of Fig. 5d, resonances associated with both the innermost (deep, broad dips) and the outermost (shallow, narrow dips) rings can be observed. Because the circumferences of the rings are different, the two types of resonances do not overlap on every free spectral range. However, when they do, a sharp spike in transmission emerges and splits the resonance. A blow up of this effect is shown in Fig. 6.

Note that the transition from the limit of weak coupling to that of strong coupling is accompanied by a halving in free spectral range (FSR), i.e., the FSR changes from about 200 MHz to 100 MHz. This occurs because, in the limit of strong coupling, the spectrum simply becomes identical to that of a ring with twice the optical path length of the individual rings. The couplings r_1 were determined by fits of Eq. (1) to the experimental data using the fixed parameters: $a_1 = 0.98, a_2 = 0.82, r_2 = 0.95$. The distinguishable point was determined from these parameters to be $r_1^{(\text{dist})} = 0.993$. The splittings of the top three curves in Fig. 5 are thus characterized as indistinguishable according to Eq. (13). This is obvious from the spectra, since for these curves the induced transparency feature never exceeds 50% of the total peak-to-valley transmission.

In summary, we experimentally demonstrated CRIT in a two coupled fiber-ring resonators. The modes can be characterized according to their degeneracy and distinguishability. Distinguishable and indistinguishable splittings were observed. Rabi oscillations are predicted for distinguishable splittings from FDTD simulations and a transient

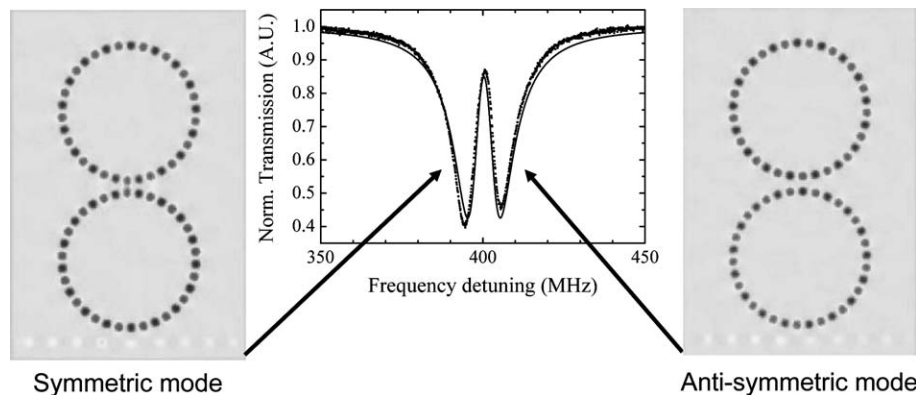


Fig. 6. A close-up view of CRIT, from Fig. 5. The solid line is a curve fit to Eq. (1) where $a_1, a_2,$ and r_1 are fitting parameters. FDTD simulations are shown for the symmetric and anti-symmetric modes after steady-state is achieved.

analysis. Narrow, sub-linewidth spectral features associated with the splitting were observed. The linewidth of the transmission peaks is determined by the coupling between the two resonators and thus could be made very small, potentially narrower than the finesse-limited resonance linewidth of the constituent resonators.

Acknowledgements

The authors acknowledge support from NASA Marshall Space Flight Center Institutional Research and Development Grants CDDF03-17 and CDDF04-08, and the United Negro College Fund Office of Special Programs.

Appendix A. Supplementary data

Supplementary data associated with this article can be found, in the online version, at [doi:10.1016/j.optcom.2006.02.037](https://doi.org/10.1016/j.optcom.2006.02.037).

References

- [1] H.A. Lorentz, *The Theory of Electrons and Its Applications to the Phenomena of Light and Radiant Heat*, Teubner, Leipzig, Germany, 1909.
- [2] W.E. Lamb, R.C. Retherford, *Phys. Rev.* 81 (1951) 222.
- [3] P.R. Hemmer, M.G.J. Prentiss, *J. Opt. Soc. Am. B* 5 (1988) 1613.
- [4] G.L. Garrido Alzar, M.A.G. Martinez, P. Nussenzeig, *Am. J. Phys.* 70 (2001) 37.
- [5] T. Opatrny, D.G. Welsch, *Phys. Rev. A* 64 (2001) 23805.
- [6] D.D. Smith, H. Chang, K.A. Fuller, A.T. Rosenberger, R.W. Boyd, *Phys. Rev. A* 69 (2004) 63804.
- [7] A.M. Akulshin, S. Barreiro, A. Lezama, *Phys. Rev. A* 57 (1998) 2996.
- [8] S.E. Harris, J.E. Field, A. Imamoglu, *Phys. Rev. Lett.* 64 (1990) 1107.
- [9] K.J. Boller, A. Imamoglu, S.E. Harris, *Phys. Rev. Lett.* 66 (1991) 2593.
- [10] A. Naweed, G. Farca, S.I. Shipova, A.T. Rosenberger, *Phys. Rev. A* 71 (2005) 043804.
- [11] L. Maleki, A.B. Matsko, A.A. Savchenkov, V.S. Ilchenko, *Opt. Lett.* 29 (2004) 626.
- [12] J.K.S. Poon, J. Scheuer, Y. Xu, A. Yariv, *J. Opt. Soc. Am. B* 21 (2004) 1665.
- [13] M.F. Yanik, S. Fan, *Phys. Rev. Lett.* 92 (2004) 083901.
- [14] M.F. Yanik, W. Suh, Z. Wang, S. Fan, *Phys. Rev. Lett.* 93 (2004) 233903.
- [15] R.J.C. Spreeuw, J.P. Woerdman, *Phys. Rev. Lett.* 61 (1988) 318.
- [16] R.J.C. Spreeuw, R. Centeno, N.J. van Druten, E.R. Eliel, J.P. Woerdman, *Phys. Rev. A* 42 (1990) 4315.
- [17] S.A. Diddams, J.C. Diels, B. Atherton, *Phys. Rev. A* 58 (1998) 2252.
- [18] R. Quintero-Torres, M. Navarro, M. Ackerman, J.C. Diels, *Opt. Commun.* 241 (2004) 179.
- [19] R.J.C. Spreeuw, N.J. van Druten, M.W. Beijersbergen, E.R. Eliel, J.P. Woerdman, *Phys. Rev. Lett.* 65 (1990) 2642.
- [20] R.J.C. Spreeuw, J.P. Woerdman, *J. Mod. Opt.* 31 (1993) 263.
- [21] D. Bouwmeester, N.H. Dekker, F.E.v. Dorsselaer, C.A. Schrama, P.M. Visser, J.P. Woerdman, *Phys. Rev. A* 51 (1995) 646.
- [22] J. Capmany, M.A. Muriel, *J. Lightwave Technol.* 8 (1990) 1904.
- [23] D.D. Smith, H. Chang, K.A. Fuller, *J. Opt. Soc. Am. B* 20 (2003) 1967.
- [24] J.K.S. Poon, J. Scheuer, S. Mookherjea, G.T. Paloczi, Y. Huang, A. Yariv, *Opt. Exp.* 12 (2004) 99.
- [25] W.D. Heiss, *J. Phys. A* 37 (2004) 2455.
- [26] W.D. Heiss, *Phys. Rev. E* 61 (2000) 929.
- [27] D.D. Smith, H. Chang, J.C. Diels, in: R.B. Lal, Donald O. Frazier (Eds.), *Proc. SPIE* 5912, San Diego, 2005.